PROTEINS: Structure, Function, and Bioinformatics 58:255–262 (2005)

SHORT COMMUNICATION

Structural Evidence for Variable Oligomerization of the N-Terminal Domain of Cyclase-Associated Protein (CAP)

Adlina Mohd Yusof,[1] Nien-Jen Hu,[1] Alexander Wlodawer,[2] and Andreas Hofmann[1]*

[1]*Institute of Structural & Molecular Biology, School of Biological Sciences, The University of Edinburgh, Scotland, United Kingdom*

[2]*Macromolecular Crystallography Laboratory, NCI at Frederick, Frederick, Maryland*

ABSTRACT **Cyclase-associated protein (CAP) is a highly conserved and widely distributed protein that links the nutritional response signaling to cytoskeleton remodeling. In yeast, CAP is a component of the adenylyl cyclase complex and helps to activate the Ras-mediated catalytic cycle of the cyclase. While the N-terminal domain of CAP (N-CAP) provides a binding site for adenylyl cyclase, the C-terminal domain (C-CAP) possesses actin binding activity. Our attempts to crystallize full-length recombinant CAP from *Dictyostelium discoideum* resulted in growth of orthorhombic crystals containing only the N-terminal domain (residues 42–227) due to auto-proteolytic cleavage. The structure was solved by molecular replacement with data at 2.2 Å resolution. The present crystal structure allows the characterization of a head-to-tail N-CAP dimer in the asymmetric unit and a crystallographic side-to-side dimer. Comparison with previously published structures of N-CAP reveals variable modes of dimerization of this domain, but the presence of a common interface for the side-to-side dimer. Proteins 2005; 58:255–262.** © **2004 Wiley-Liss, Inc.**

Key words: ASP-56; CAP; crystal structure; MCH1; protein crystallography; protein–protein interactions; Srv2

INTRODUCTION

A large number of motile and morphogenetic processes in eukaryotic cells are dependent on the assembly and rapid turnover of highly dynamic filaments of the actin cytoskeleton. The actual state of these filaments as constituted by form, dynamics, localization, and mechanical properties is regulated by a number of actin-binding proteins which, in turn, are controlled by various signaling pathways. One family of conserved eukaryotic proteins regulating actin dynamics is the cyclase-associated proteins (CAPs). In *Saccharomyces cerevisiae*, these proteins copurify with adenylyl cyclase[1] and were identified as a suppressor of the activated *ras* allele.[2,3] It is now generally accepted that CAP determines cell polarity and affects development (for a recent review see Hubberstey and Mottillo[4]).

In yeast, CAP (alias Srv2) localizes to the cortical actin patches, via interaction with actin filament binding protein 1 (Abp1p).[5,6] Deletion of CAP in yeast,[7,8] *Drosophila melanogaster*[9–11] and *Dictyostelium discoideum*[12,13] generally results in developmental defects. At the molecular level, it has been shown for *Dictyostelium* and yeast that CAP is needed for adenylyl cyclase activity.[13] Full-length CAP constitutes an N-terminal domain, required for Ras response,[7] a C-terminal domain that interacts with the cytoskeleton, and a middle domain harboring two proline-rich regions (mammalian CAPs only).

Biochemically and genetically, it has been shown in *S. cerevisiae* that the N-terminal 36 residues of CAP bind to the C-terminal domain of adenylyl cyclase, presumably by coiled-coil interactions.[14] A recent study of a *Dictyostelium* knockout mutant also suggested an interaction of CAP with adenylyl cyclase.[13] The catalytic activity of the cyclase is activated by Ras binding, which is facilitated by CAP, probably by providing a binding site for the Ras farnesyl group.[15] The adenylyl cyclase binding site in the mammalian homologues of CAP is conserved, although they do not interact with the cyclase directly due to the lack of a CAP-binding domain in the mammalian cyclases.[16] Meanwhile, in all the CAP homologues studied so far, the C-terminal domain has been reported to bind actin monomers.[7,16–21]

To date, there has been no evidence for the existence of multiple CAP genes in nonmammalian species. However,

This paper is dedicated to Helma Hofmann on the occasion of her 60th birthday.

Since this article went to press, the crystal structure of C-CAP has been published by Dodatko and colleagues in Biochemistry 2004;43: 10628–10641.

*Correspondence to: Andreas Hofmann, Institute of Structural & Molecular Biology, School of Biological Sciences, The University of Edinburgh, The King's Buildings, Mayfield Road, Edinburgh EH9 3JR, Scotland, UK. E-mail: Andreas.Hofmann@ed.ac.uk

Received 23 June 2004; Accepted 28 July 2004

Published online 19 November 2004 in Wiley InterScience (www.interscience.wiley.com). DOI: 10.1002/prot.20314

in mammals, at least two CAP gene products (CAP1 and CAP2) share about 64% identity.[4] In a recent study, CAP1 was found to be expressed in the non-muscle cells of mice, while CAP2 is only expressed in striated muscles and certain brain regions.[22] Furthermore, using CAP1 knockout cells, the authors observed that CAP1 promotes rapid actin filament depolymerization, and is required for proper subcellular localization and function of actin-deploymerizing factor (ADF)/cofilin. These results agree with earlier studies[6,23] and a functional CAP model has been proposed where the N-terminal domain of CAP1 acts, together with cofilin, as an accelerator of F-actin depolymerization at the pointed end of actin filaments. Likewise, the C-terminal domain of CAP1 is involved in filament elongation at the barbed end. The role of CAP1 in actin filament turnover thus appears to be the efficient recycling of cofilin and actin. Apparently, the view of CAP as a bifunctional protein, with the N-terminal domain responsible for proper signal transduction and the C-terminal domain involved in cytoskeletal dynamics, seems to be oversimplified. Now, there is evidence that the N-terminal domain of CAP interacts with the actin:cofilin complex, while the C-terminal domain interacts with F-actin.[23] An important role is also inferred for the proline-rich middle region, which might act in combination with the N- or C-terminal domain.[13]

Early on, a functional link between CAP and profilin had been proposed for CAP from *S. cerevisiae*.[8] A study using human CAP constructs indicated that profilin II can interact with the proline-rich domain of CAP.[24] For *Dictyostelium* CAP, this interaction seems rather unlikely due to the degeneration of the proline-rich sequence in the middle domain. For yeast CAP, it has been reported that this middle region acts as a binding site for SH3 domains[25] and access to the SH3 binding motif directs the subcellular translocation of CAP.[16,21] It is thus tempting to speculate a structural model of CAP, where the protein can adopt varying conformations with different arrangements of the N- and C-terminal domains with respect to each other, thereby exposing or preventing access to the middle domain. In a mechanism yet to be clarified, these conformations include the formation of CAP homo-oligomers.

Despite the wealth of information about the biological implications of CAP, little is known about its molecular mechanisms. Several crystal structures of CAP C-terminal domains have been solved by Almo and colleagues, and are available in the PDB (yeast: 1f5i, 1k4z, 1kq5; human: 1k8f). C-CAP adopts a β helix structure, a fold built solely by parallel β-strands arranged in a right-handed helical manner. Notably, all structures have been found to be dimeric in the crystals. Recently, the X-ray crystal structure[26] and the NMR structure[27] of an N-terminal CAP construct have been determined. In contrast to C-CAP, N-CAP adopts an all-α-helical fold where six helices are arranged in an anti-parallel fashion to yield a six-helix-bundle protein. The NMR and X-ray structures provide consistent data on the conformation of the monomeric protein. In the X-ray structure paper, the authors reported two crystal forms, which contain either a monomer or dimer of N-CAP, respectively.[26] They put forward a hypothesis that a magnesium ion is responsible for the dimerization of the N-terminal domain, although they could not present convincing evidence nor corroborate the finding in their second study.

TABLE I. Data Collection Statistics†

Data set	CC1
Space group	$C222_1$
Unit-cell parameters (Å)	71.2, 75.1, 162.9
Resolution (Å)	20–2.2
Number of measurements[a]	313526
Number of independent reflections	21214 (2987)
Multiplicity	6.0 (5.6)
Completeness	0.988 (0.943)
R_{merge}[b]	0.072 (0.303)

†Values in parentheses refer to the last resolution shell.
[a]Including partial reflections.
[b]$R_{merge} = \Sigma I|-\langle|\rangle|I/\Sigma I$

Previously, we have reported the crystallization and X-ray diffraction of a protein obtained from the expression of full-length *D. discoideum* CAP.[28] Structural studies on full-length CAP have been hampered by the notoriously difficult behavior of the protein, which apparently possesses auto-proteolytic activity apart from having the tendency to precipitate at high concentrations in the presence of membranes.

In this paper, we report the X-ray crystal structure of N-CAP obtained from the auto-proteolytic fragments of the full-length protein from *D. discoideum*. The structure reveals the six-helix-bundle fold in agreement with previous studies. However, in the present structure, two different N-CAP dimers are observed, a side-to-side dimer similar to the one reported by Holak and coworkers,[26] and a previously unknown head-to-tail dimer. The study also provides evidence that N-CAP dimer formation is independent of magnesium and that the protein is able to engage in a variety of homo-oligomerization modes.

MATERIALS AND METHODS

Crystallization and Data Collection

As described previously,[28] crystal growth in slightly basic ammonium sulfate conditions (1.8 M $(NH_4)_2SO_4$, 0.1 M TRIS, pH 8.4) occurs after about seven to eight months and yields only a few crystals suitable for X-ray diffraction. The best crystal we obtained so far diffracted to 2.2 Å and was used to acquire data set CC1.

The X-ray data collected in-house was initially processed in space group C222, since no clear distinction could be made between C222 and $C222_1$ based on an extinction pattern of 00*l* reflections. Subsequent structure solution with molecular replacement methods clearly indicated that $C222_1$ is the final space group. The data was thus reprocessed with *MOSFLM*.[29] Scaling, merging, and truncation were performed with programs from the CCP4 suite.[30] The final data collection statistics are shown in Table I.

Structure Solution, Model Building, and Refinement

The structure was solved by molecular replacement using *AMoRe*[31] and the model of N-CAP (PDB entry 1s0p).

TABLE II. Refinement Statistics[†]

	Total	Molecule 1	Molecule 2
Refinement			
Resolution (Å)	2.2		
Number of reflections used for refinement (F > 0)	21214 (3062)		
Number of non-H atoms	3169	1595	1574
Number of non-H protein atoms	2860	1431	1429
Visible residues		43–227	42–227
R-factor			
Number of reflections in working set	19114 (2734)		
Number of reflections in test set	2100 (328)		
R[a]	0.196 (0.222)		
R_{free}[b]	0.244 (0.287)		
Temperature factors			
Scaling	Anisotropic		
Average B-factor (Å^2)	36.4	35.3	37.5
RMS deviation for bonded atoms (Å^2)	2.63	2.65	2.62
Geometry RMS deviations			
Bond lengths (Å)	0.011		
Bond angles (°)	1.40		
Dihedral angles (°)	19.5		
Improper angles (°)	0.97		
Ramachandran plot			
Most favored (%)	91.8	90.9	92.7
Additionally allowed / generously allowed / disallowed (%)	7.6 / 0.6 / 0	9.1/0/0	6.1/1.2/0
Solvent statistics			
Number of water molecules	279	144	135
Number of sulphate ions	6	4	2

[†]Values in parentheses refer to the last resolution shell.
[a]R factor = $\Sigma||F_o| - |F_c||/\Sigma|F_o|$, where F_o and F_c are the observed and calculated structure factors, respectively.
[b]R_{free} defined in Brunger.[41].

Initially, four N-CAP molecules could be located in space group C222. Close inspection of the packing revealed the presence of a 2_1 axis parallel to z. In C222$_1$, a clear solution was found for two molecules in the asymmetric unit with correlation coefficients of 38.8 and 59.6 for the first and second molecule, respectively (R factor: 0.496 and 0.410).

The initial model was rebuilt with the program O[32] and subjected to several cycles of computational refinement interspersed with visual inspection and manual adjustments. Refinement was carried out using the conjugate gradient method with *CNS* v.1.0[33] and a maximum likelihood target function. Typical protocols consisted of a positional refinement followed by simulated annealing, grouped and individual B-factor refinement, and a final positional refinement. A bulk solvent model and overall anisotropic B-factor correction (B_{11} = 1.41, B_{22} = 9.29, B_{33} = −10.70, B_{12} = 0, B_{13} = 0, B_{23} = 0) were applied throughout the procedure. The structure was refined to a final R factor of 0.196 (R_{free} = 0.244) and proper geometry was monitored with the program *PROCHECK*.[34] Refinement statistics are summarized in Table II. The side chains of two residues in molecule 1 (Glu107, Glu111) and five residues in molecule 2 (Glu107, Lys203, Lys206, Thr226, Pro227), which could not be located due to poor electron density, were modeled with Ala. The coordinates and structure factors have been deposited with the PDB (accession number 1tjf).

RESULTS

Crystal Packing

Initially, when we tried to solve the structure with the assumption that the crystal contains full-length CAP, the lack of success quickly proved otherwise. Using the model of the N-terminal domain of CAP with Patterson search methods, we were able to localize two molecules of N-CAP in the asymmetric unit.

In the space group C222$_1$, where the crystallographic 2_1 axis runs parallel to the z direction, the two molecules in the asymmetric unit are grouped around the 2_1 axis and shifted by 40 Å in the z direction. Application of the 2_1 symmetry operator creates another dimer shifted by 83 Å in the z direction [Fig. 1(A)]. This results in an arrangement of four protein molecules around a rotation axis parallel to z, where the operation needed to transform one molecule into the next is a rotation of 90° and a subsequent translation along z by about ¼ c [Fig. 1(B)]. Thus, the packing in the present crystal structure has a pseudo-4_1 axis superimposed on the 2_1 symmetry operator. Crystallization in a different space group, such as P4$_1$22, is hindered by the fact that the pseudo-4_1 axes calculated from the first and the second asymmetric dimer are tilted against each other by 1.5°. The R_{merge} for processing the data in P4$_1$22 yielded 0.154, highlighting the level of imperfection of the pseudo-4_1 arrangement. Nevertheless, the presence of this pseudo symmetry element is also visible from the extinction pattern in the 00l reflections (Fig. 2).

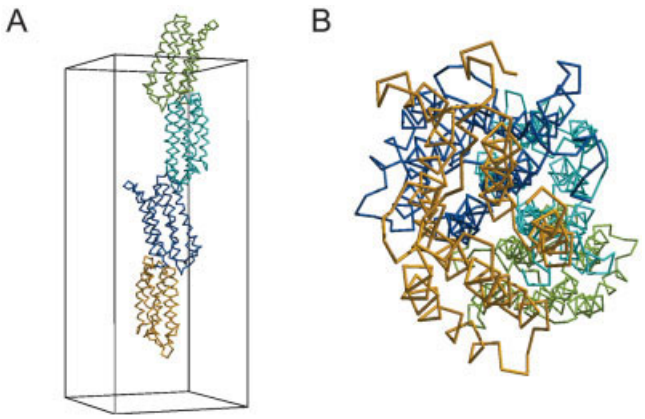

Fig. 1. The crystal packing. **A**: View of the asymmetric dimer and its symmetry mate generated by the crystallographic 2_1 operation. **B**: View along the pseudo-4_1 axis. The 4_1 operation transforms the yellow molecule into the blue molecule, and subsequently into the cyan and green molecule. Figure was prepared with *MOLSCRIPT*/*BOBSCRIPT*,[37,38] and rendered with *Raster3D* and *POVRay*.[39,40]

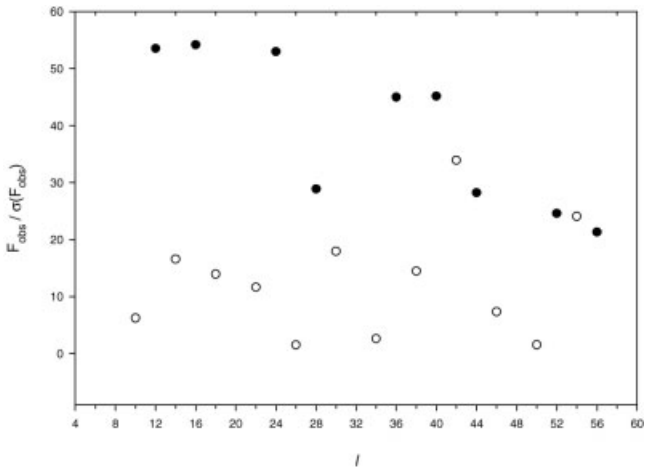

Fig. 2. Extinction pattern in the 00*l* reflections. Shown are the $F_{obs}/\sigma(F_{obs})$ values for 00*l* reflections. Two extinction patterns are superimposed: patterns for $l = 4n$ (closed circles; pseudo-4_1 axis) and $l = 2n$ (open circles; 2_1 axis) are clearly visible.

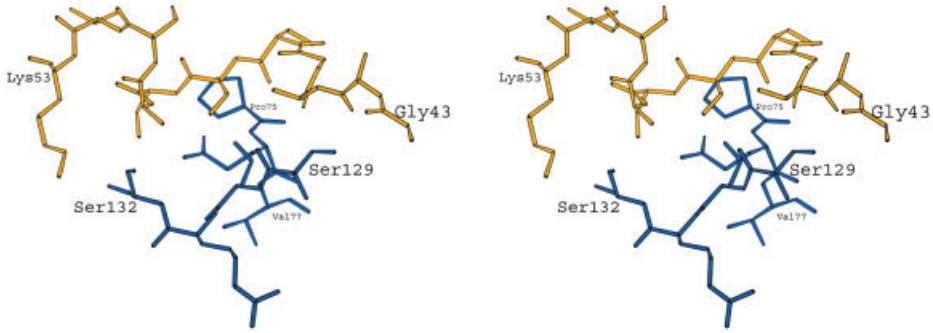

Fig. 3. Interaction interface of the orthorhombic head-to-tail dimer (stereo figure). The dimer within the asymmetric unit is formed by interactions between the loops connecting helices α1/α2 and α3/α4 in molecule 1 (blue) and the N-terminal tail region in molecule 2 (yellow). Figure was prepared with *BOBSCRIPT*.[38]

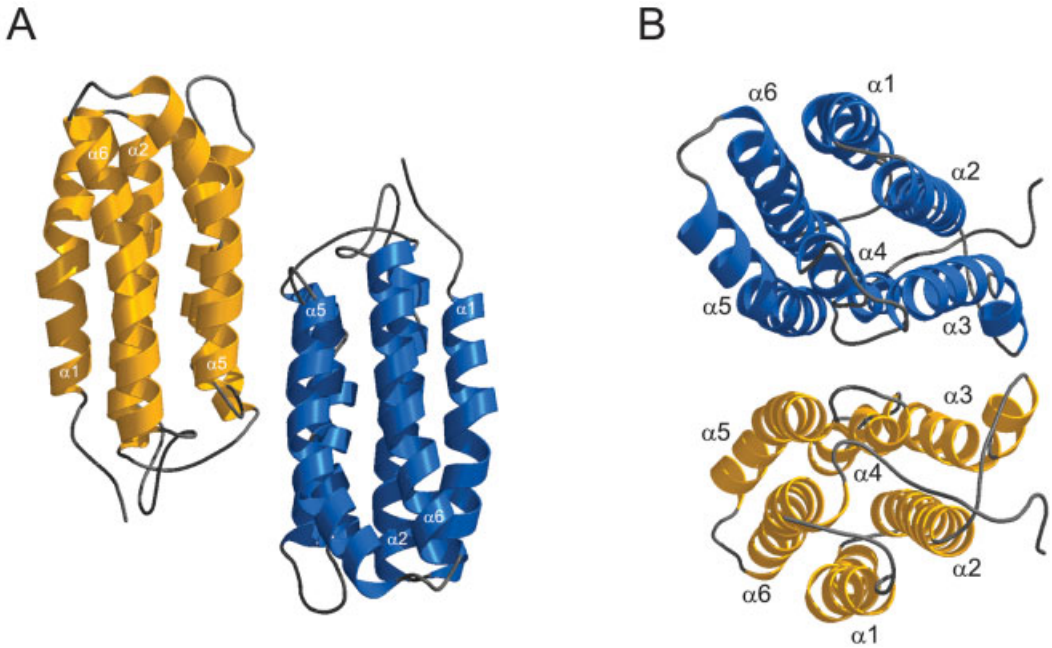

Fig. 4. The orthorhombic side-to-side dimer. Two crystallographically related N-CAP molecules are organized to yield an anti-parallel side-to-side dimer with the contact interface provided mainly by helices α3 and α5. **A**: The view parallel to the dimer interface. **B**: View along the two-fold rotation axis. Figure was prepared with *BOBSCRIPT*[38] and rendered with *POVRay*.[40]

TABLE III. Structural Alignment†

Molecule 1 versus	Positional RMS (Å)	RMS ΔB (Å^2)
Molecule 2	0.84	6.96
1s0p (Molecule 1)	1.12	15.5

†Calculations were performed with the program *ALIGN*[42] using all atoms.

Overall Structure

The visible residues in the present structure extend from 43 to 227 (molecule 1) and from 42 to 227 (molecule 2), respectively. At the N-terminal side of helix α1, residues 43 to 51 adopt a coil conformation in our structure. There is no interpretable electron density from residues 1 to 42, although the packing provides enough space to accommodate these residues. Similarly, the exact determination of the last C-terminal residue was not possible because the electron density does not extend beyond residue 227.

The absence of interpretable density from residues 1 to 42 might indicate that the beginning of the N-terminal CAP domain is not structured or that it is a very flexible part of the protein. Alternatively, it is possible that this peptide sequence was cleaved, making the crystallized protein N-terminally truncated. It is interesting to note that Holak and coworkers[27] did observe the truncation of an N-terminal CAP construct between residues 50 and 51. The recently published NMR structure of N-CAP indicates that even with the intact N-terminal domain, the first 50 residues might fold only when they are engaged in interactions with a binding partner. Since mass spectrometry analysis of the X-rayed crystals was unsuccessful,[28] the actual length of the crystallized protein in this study could not be determined.

The structure of the N-terminal domain of CAP as determined in this study agrees well with the N-CAP structures reported earlier.[26,27] This is evident from the root-mean-square deviation (RMSD) between our structure and 1s0p (Table III). N-CAP comprises six anti-parallel α-helices and adopts the fold of a helix-bundle of about 50 Å in length and 20 Å in diameter. The six helices contain about 22 amino acids each and four of them show a significant kink (helix α1 at Gln61, helix α3 at Ile113, helix α4 at Ser143 and helix α5 at Thr173). According to *B*-factor analysis, the protein possesses flexible regions, especially the loop between helices α5 and α6 (residues 180–185), the extreme C-terminal area (residues 221–227) and the first half of helix α3 (residues 106–120).

Comparison of N-CAP Dimers

The $C222_1$ structure of N-CAP as reported here provides new insights into N-CAP dimer formation because two different dimer interactions can be characterized. First, there is the dimer in the asymmetric unit (head-to-tail dimer), whose contact interface is provided by the loops connecting helices α1/α2 and α3/α4 (head) in molecule 1 and by the N-terminal tail region in molecule 2 (Fig. 3). Protein–protein interactions for this dimer are direct interactions either between side chains or between backbone carbonyl groups and side chains (Table IV). A second dimer (side-to-side dimer) is formed in $C222_1$ by the interactions between one molecule of the asymmetric dimer and a crystallographic symmetry mate (Fig. 4). In contrast to the other dimer, the dimer interface in this case does not show direct contacts between residues from each monomer. Calculations of buried surface areas indicate that the side-to-side dimer possesses an interface of about 10% of the monomer surface, compared to the head-to-tail dimer interface which is only about 7% (Table V).

Ksiazek and colleagues[26] reported the structure of recombinant N-CAP where only that domain was expressed (PDB entry 1s0p). The authors found crystals belonging to two different space groups, P1 and $P2_1$. The P1 crystals contained a side-to-side N-CAP dimer in the asymmetric unit with an anti-parallel arrangement of the two helix-

TABLE IV. Comparison of the Dimer Interfaces for $C222_1$ and P1†

	$C222_1$ dimers		P1 dimer
Molecule #1	Head-to-tail dimer	Side-to-side dimer	Side-to-side dimer
Contacting residues (distance < 3.2 Å)			
CO43	S129		
CO44	S129		
CO47	E76		
S48	E76		
S48	N130		
S49	E76		
K53	CO132		
Q106		N117, N118	
Nearest neighbors (distance: 3.2 Å–4 Å)			
R131			R117
CO144		P156	
V154		M165	
P156		CO144, S168	
T157		M165, S168	
P160		E164	
H161		H161	F171, R175
E164		P160	CO167, S168
M165		CO155	F171, Y172
CO167			E164
S168		T157, P156	E164, S168
F171			H161, M165
Y172			M165
R175			H161

†Contacting residues and nearest neighbors identified within the dimer interfaces. Residues in bold are part of the dimer interface in both structures.

TABLE V. Buried Surface Areas of the N-CAP Dimers†

	$C222_1$ dimers		P1 dimer
	Head-to-tail dimer	Side-to-side dimer	Side-to-side dimer
Buried surface area (Å^2)	1219	1744	1934
Fraction of monomer (%)	7	10	10

†Buried surface areas as calculated with a 2-Å probe with CNS.[33]

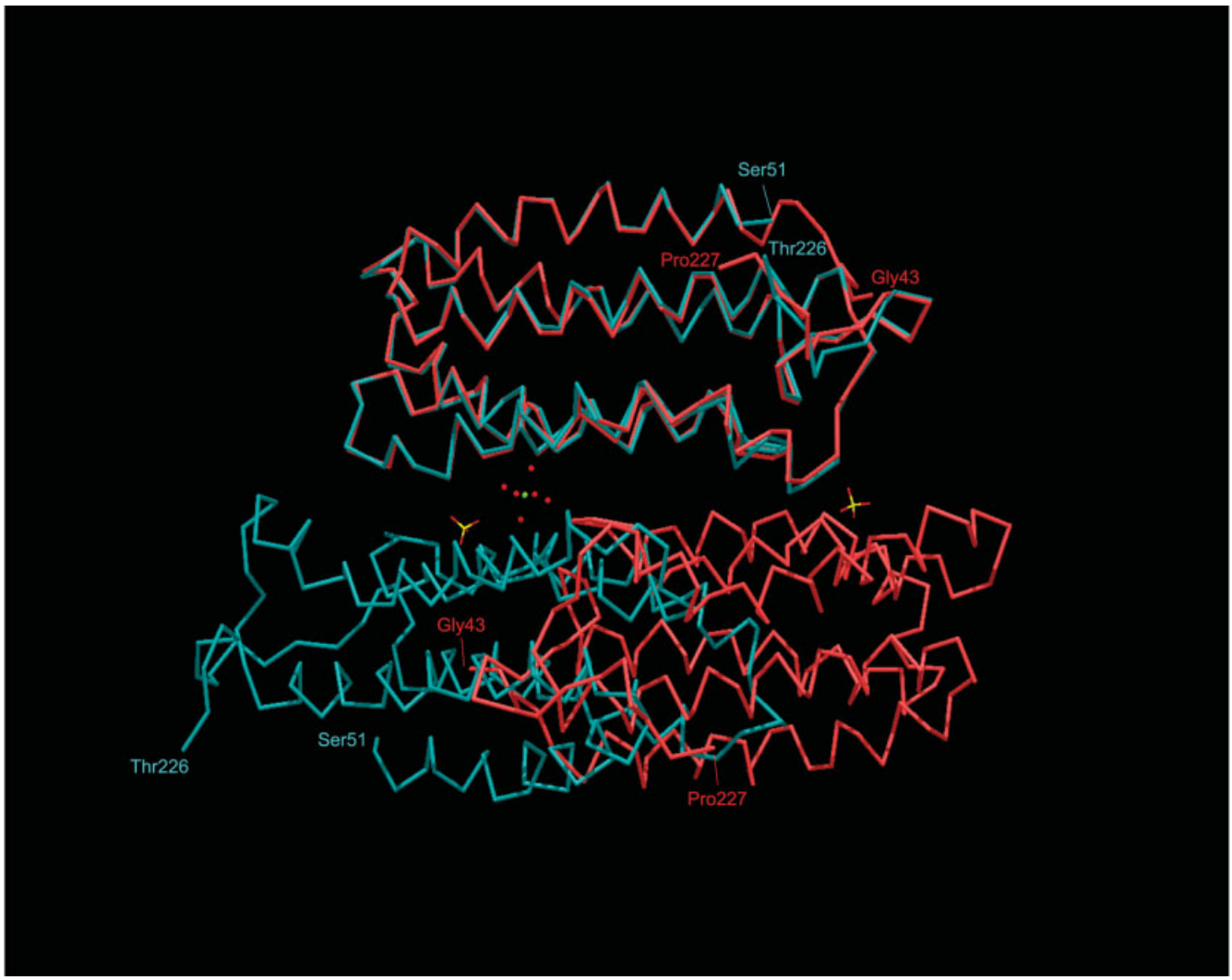

Fig. 5. Superposition of the orthorhombic and triclinic side-to-side dimers. Molecule 1 of the side-to-side dimer of our structure and the triclinic N-CAP structure (1s0p)[26] are aligned. The Cαtrace of our structure (red) and the dimer from 1s0p (cyan) are shown. Explicitly depicted are the hexa-aqua-Mg^{2+} complex of 1s0p and two sulfate ions close to the dimer interface in the present structure. Figure was prepared with *BOBSCRIPT*[38] and rendered with *POVRay*.[40]

bundle proteins. The dimer interface of the P1 structure, provided by helices α3 and α4 of two adjacent molecules, has a mainly hydrophobic nature. The authors claim that a Mg^{2+} ion coordinated in this interface by residues Asp128, Arg127, Glu144, Glu144′, Arg127′ and Asp128′ is responsible for the dimerization, although no supporting evidence was presented.

When superimposing the side-to-side dimer from $C222_1$ with the P1 dimer (Fig. 5), it becomes obvious that although the quaternary structures are different, several features are common in both conformations. Compared to the anti-parallel arrangement of the monomers in the P1 dimer, the $C222_1$ dimer adopts a conformation where the second molecule is shifted alongside the first molecule, also resulting in an anti-parallel arrangement (Fig. 5). Both dimer interfaces are located at the same side of N-CAP, involving the surfaces of helices α3, α4, and α5. Only one direct interaction of side chains between the two monomers could be identified in our structure (Gln106-Asn117/Asn118), whereas the P1 dimer exclusively interacts via water molecules. Residues in the interface of both dimers are mainly hydrophobic and there is a file of water molecules running through both interfaces. In an attempt to further characterize the dimers, we analyzed the nearest residues within both interfaces using a cutoff distance of 4 Å. A summary of this analysis is given in Table IV. Five residues were found to be a part of the dimer interface in both structures: His161, Glu164, Met165, Ser168, and Phe171.

While a special feature of the P1 dimer is the coordination of a hexa-aqua-Mg^{2+} complex within the dimer interface, our structure shows the presence of a sulfate ion. The sulfate is provided by the precipitant used for crystallization and is found in the vicinity of residues Ser105 and Gln106 within the interface of the $C222_1$ dimer. Notably, there is also a sulfate ion close to the site where the hexa-aqua-Mg^{2+} complex is bound in the P1 structure

(Arg127, Arg131). Coordination of the sulfate ions by protein residues is only indirect via water molecules.

DISCUSSION

Findings from the present study allow valuable insights into the oligomerization behavior of CAP. A previous report concluded that Mg^{2+} is responsible for the dimerization of N-CAP thus implying that there is only one specific N-CAP dimer conformation.[26] Our orthorhombic structure of N-CAP reveals two dimer conformations: a head-to-tail dimer with a slightly smaller interface and a side-to-side dimer similar to the one previously reported. Comparison of the side-to-side dimers from the orthorhombic and triclinic crystal structures[26] shows that, although the conformations are different, there exists a common interface mainly provided by the surface of helix α5.

The interface area of the side-to-side dimers is larger than that of the head-to-tail dimer (Table V). The fact that the side-to-side dimers have been observed in two different space groups leads us to assume that these are not crystallization artifacts. Furthermore, in a survey of buried surface areas of structures in the PDB, Janin[35] came to the conclusion that complexes with an interface area of more than 700 Å are very likely to be significant, that is, they are not just crystallization artifacts. With N-CAP, the interface area of the side-to-side dimers is about 10% (approximately 900 $Å^2$ per monomer) of the entire monomer surface, which makes the biological significance of this dimerization quite likely. For comparison, the head-to-tail dimer possesses a smaller interface area of about 7% (approximately 600 $Å^2$ per monomer) which, according to Janin, is less than the threshold for a biologically significant dimerization. Notably, the interactions in the head-to-tail dimer interface are direct interactions between the side chains and backbone carbonyl groups of the two monomers. Therefore, these interactions are stronger than the nonspecific interactions of the side-to-side dimer. Based on this crystallographic analysis, the side-to-side dimer of N-CAP might be biologically important, whereas the head-to-tail dimer is less likely to occur in solution.

It has been reported that CAP can form multimeric complexes with itself, whereby the N-terminal domain is able to interact with either the N-terminal domain[16] or the C-terminal domain[20] of a second CAP molecule. Similarly, the C-terminal domain of one CAP molecule can also interact with the C-terminal domain of another.[20] To date, albeit a single multimerization motif has not been identified, Yu and coworkers[16] have reported three N-terminal mutants with decreased multimerization tendencies (L16P, R19T, L27F; residue numbers for Srv2). Their data support the earlier hypothesis that the N-terminal region of CAP contains a site responsible for multimerization.[20,21] However, there is no structural data available which would allow further conclusions.

There is now structural evidence based on this study showing that N-CAP can engage in at least two modes of intermolecular interactions, although the entire N-terminal domain possesses at least three different interaction sites for multimerization. Additionally, the existence of at least two conformations of N-CAP side-to-side dimers emphasizes the high degree of variability inherent in this protein. At the molecular level, this variability is most likely due to the nonspecific, "shape-determined" interactions within the dimer interface. This complex situation is mirrored by observations of CAP in solution, which indicate the presence of hexamers.[26] Therefore, we would like to hypothesize that, in the absence of its physiological binding partners, CAP oligomers might lack a required element of organization, thus allowing the molecules to engage in nonspecific associations. This hypothesis is supported by the high tendency of the full-length protein to precipitate above a certain concentration (Mohd Yusof et al., unpublished).

The variable conformations of the side-to-side dimers of N-CAP, a helix-bundle protein, are also interesting from a topological point of view. This is because the crystal structures of GFP, a β-barrel protein, have revealed different dimer conformations.[36] The cylindrical shape of barrel and bundle proteins seems to foster the formation of variable protein–protein interactions, probably because the protein surface appears rather smooth compared to other globular folds with distinct domains or structural features.

Recently, we reported for the first time that recombinant full-length CAP undergoes self-cleavage, irrespective of the presence of protease inhibitors, rendering mixtures of unprocessed full-length CAP, N-CAP, and C-CAP (starting at residue 279).[28] Subsequent publications on CAP mention that an N-terminal construct of CAP (residues 1–226) is processed, even in the presence of protease inhibitors, and the degradation products lack the extreme N-terminal region (residues 1–53, 1–50, 1–48, 1–43).[27] To date, the mechanisms of CAP auto-proteolysis remain unclear. However, these observations emphasize the importance of the physiological binding partners of CAP for its function, and probably for the investigation of its molecular mechanisms, since complexes comprising full-length CAP might increase the stability of this protein.

CONCLUSION

With the availability of the three-dimensional structures of N- and C-terminal domains of CAP, first insights into the molecular properties of this important protein have become accessible. Correlating the structural findings with biochemical/cell biological data, it is clear that CAP can employ variable modes of homo-oligomerization. Although the crystal structures have only revealed interactions of the same domains (N-CAP/N-CAP or C-CAP/C-CAP), it is possible that the protein can also engage in other interactions such as N-CAP/C-CAP (see also Hubberstey and Mottillo[4]). Therefore, further studies will be necessary to elucidate the complex molecular mechanisms of this protein.

ACKNOWLEDGMENTS

We gratefully acknowledge financial support for this study by the BBSRC. We thank Angelika A. Noegel and Michael Schleicher for their collaboration, and Tad Holak

for making the coordinates of N-CAP available at an early stage.

REFERENCES

1. Field J, Nikawa J, Broek D, MacDonald B, Rodgers L, Wilson I, Lerner R, Wigler M. Purification of a RAS-responsive adenylyl cyclase complex from *Saccharomyces cerevisiae* by use of an epitope addition method. Mol Cell Biol 1988;8:2159–2165.
2. Fedor-Chaiken M, Deschenes R, Broach J. SRV2, a gene required for RAS activation of adenylate cyclase in yeast. Cell 1990;61:329–340.
3. Field J, Vojtek A, Ballester R, Bolger G, Colicelli J, Ferguson K, Gerst J, Kataoka T, Michaeli T, Powers S. Cloning and characterization of CAP, the *S. cerevisiae* gene encoding the 70 kd adenylyl cyclase-associated protein. Cell 1990;61:319–327.
4. Hubberstey AV, Mottillo EP. Cyclase-associated proteins: CAPacity for linking signal transduction and actin polymerization. FASEB J 2002;16:487–499.
5. Lila T, Drubin D. Evidence for physical and functional interactions among two Saccharomyces cerevisiae SH3 domain proteins, an adenylyl cyclase-associated protein and the actin cytoskeleton. Mol Biol Cell 1997;8:367–385.
6. Balcer H, Goodman A, Rodal A, Smith E, Kugler J, Heuser J, Goode B. Coordinated regulation of actin filament turnover by a high-molecular-weight Srv2/CAP complex, cofilin, profilin, and Aip1. Curr Biol 2003;13:2159–2169.
7. Gerst J, Ferguson K, Vojtek A, Wigler M, Field J. CAP is a bifunctional component of the *Saccharomyces cerevisiae* adenylyl cyclase complex. Mol Cell Biol 1991;11:1248–1257.
8. Vojtek A, Haarer B, Field J, Gerst J, Pollard TD, Brown S, Wigler M. Evidence for a functional link between profilin and CAP in the yeast *S. cerevisiae*. Cell 1991;66:497–505.
9. Baum B, Li W, Perrimon N. A cyclase-associated protein regulates actin and cell polarity during *Drosophila* oogenesis and in yeast. Curr Biol 2000;10:964–973.
10. Benlali A, Draskovic I, Hazelett D, Treisman J. Act up controls actin polymerization to alter cell shape and restrict Hedgehog signaling in the *Drosophila* eye disc. Cell 2000;101:271–281.
11. Baum B, Perrimon N. Spatial control of the actin cytoskeleton in *Drosophila* epithelial cells. Nat Cell Biol 2001;3:883–890.
12. Noegel AA, Rivero F, Albrecht R, Janssen KP, Kohler J, Parent CA, Schleicher M. Assessing the role of the ASP56/CAP homologue of *Dictyostelium discoideum* and the requirements for subcellular localization. J Cell Sci 1999;112:3195–3203.
13. Noegel AA, Blau-Wasser R, Sultana H, Muller R, Israel L, Schleicher M, Patel H, Weijer CJ. The cyclase-associated protein CAP as regulator of cell polarity and cAMP signaling in *Dictyostelium*. Mol Biol Cell 2004;15:934–945.
14. Nishida Y, Shima F, Sen H, Tanaka Y, Yanagihara C, Yamawaki-Kataoka Y, Kariya K, Kataoka T. Coiled-coil interaction of N-terminal 36 residues of cyclase-associated protein with adenylyl cyclase is sufficient for its function in *Saccharomyces cerevisiae* ras pathway. J Biol Chem 1998;273:28019–28024.
15. Shima F, Yamawaki-Kataoka Y, Yanagihara C, Tamada M, Okada T, Kariya K, Kataoka T. Effect of association with adenylyl cyclase-associated protein on the interaction of yeast adenylyl cyclase with Ras protein. Mol Cell Biol 1997;17:1057–1064.
16. Yu J, Wang C, Palmieri SJ, Haarer BK, Field J. A cytoskeletal localizing domain in the cyclase-associated protein, CAP/Srv2p, regulates access to a distant SH3-binding site. J Biol Chem 1999;274:19985–19991.
17. Kawamukai M, Gerst J, Field J, Riggs M, Rodgers L, Wigler M, Young D. Genetic and biochemical analysis of the adenylyl cyclase-associated protein, CAP, in *Schizosaccharomyces pombe*. Mol Biol Cell 1992;3:167–180.
18. Freeman NL, Chen Z, Horenstein J, Weber A, Field J. An actin-monomer binding activity localises to the carboxyl-terminal half of the *Saccharomyces cerevisiae* cyclase-associated protein. J Biol Chem 1995;270:5680–5685.
19. Gottwald U, Brokamp R, Karakesisoglou I, Schleicher M, Noegel AA. Identification of a cyclase-associated protein (CAP) homologue in Dictyostelium discoideum and characterization of its interaction with actin. Mol Biol Cell 1996;7:261–272.
20. Hubberstey A, Yu G, Loewith R, Lakusta C, Young D. Mammalian CAP interacts with CAP, CAP2, and actin. J Cell Biochem 1996;61:459–466.
21. Zelicof A, Protopopov V, David D, Lin X, Lustgarten V, Gerst J. Two separate functions are encoded by the carboxyl-terminal domains of the yeast cyclase-associated protein and its mammalian homologs. Dimerization and actin binding. J Biol Chem 1996;271:18243–18252.
22. Bertling E, Hotulainen P, Mattila PK, Matilainen T, Salminen M, Lappalainen P. Cyclase-associated protein 1 (CAP1) promotes cofilin-induced actin dynamics in mammalian nonmuscle cells. Mol Biol Cell 2004;15:2324–2334.
23. Moriyama K, Yahara I. Human CAP1 is a key factor in the recycling of cofilin and actin for rapid actin turnover. J Cell Sci 2002;115:1591–1601.
24. Lambrechts A, Verschelde J, Jonckhere V, Goethals M, Vandekerckhove J, Ampe C. The mammalian profilin isoforms display complementary affinities for PIP_2 and proline-rich sequences. EMBO J 1997;16:484–494.
25. Freeman NL, Lila T, Mintzer KA, Chen Z, Pahk AJ, Ren R, Drubin DG, Field J. A conserved proline-rich region of the Saccharomyces cerevisiae cyclase-associated protein binds SH3 domains and modulates cytoskeletal localization. Mol Cell Biol 1996;16:548–556.
26. Ksiazek D, Brandstetter H, Israel L, Bourenkov GP, Katchalova G, Janssen KP, Bartunik HD, Noegel AA, Schleicher M, Holak TA. Structure of the N-terminal domain of the adenylyl cyclase-associated protein (CAP) from *Dictyostelium discoideum*. Structure 2003;11:1171–1178.
27. Mavoungou C, Israel L, Rehm T, Ksiazek D, Krajewski M, Popowicz G, Noegel AA, Schleicher M, Holak TA. NMR structural characterization of the N-terminal domain of the adenylyl cyclase-associated protein (CAP) from *Dictyostelium discoideum*. J Biomol NMR 2004;29:73–84.
28. Hofmann A, Hess S, Noegel AA, Schleicher M, Wlodawer A. Crystallization of cyclase-associated protein from *Dictyostelium discoideum*. Acta Crystallogr D Biol Crystallogr 2002;58:1858–1861.
29. Leslie A. MOSFLM. 6.2.3. Cambridge, UK: Medical Research Council, Laboratory of Molecular Biology; 2003.
30. Collaborative Computational Project N. The CCP4 suite: programs for protein crystallography. Acta Crystallogr D Biol Crystallogr 1994;50:760–763.
31. Navaza J. Implementation of molecular replacement in AMoRe. Acta Crystallogr D Biol Crystallogr 2001;57:1367–1372.
32. Jones T, Zou J, Cowan S, Kjeldgaard M. Improved methods for building protein models in electron density maps and location of errors in these models. Acta Crystallogr A Found Cryst 1991;47:110–119.
33. Brünger A, Adams P, Clore G, Delano W, Gros P, Grosse-Kunstleve R, Jiang J, Kuszewski J, Nilges N, Pannu N, Read R, Rice L, Simonson T, Warren G. Crystallography and NMR system (CNS): a new software system for macromolecular structure determination. Acta Crystallogr D Biol Crystallogr 1998;54:905–921.
34. Laskowski R, MacArthur M, Moss D, Thornton J. PROCHECK: A program to check the stereochemical quality of protein structures. J Appl Cryst 1993;26:283–291.
35. Janin J. Specific *versus* non-specific contacts in protein crystals. Nat Struct Biol 1997;4:973–974.
36. Hofmann A, Iwai H, Hess S, Plückthun A, Wlodawer A. Structure of cyclized green fluorescent protein. Acta Crystallogr D Biol Crystallogr 2002;58:1400–1406.
37. Kraulis P. MOLSCRIPT: A program to produce both detailed and schematic plots of protein structures. J Appl Cryst 1991;24:946–950.
38. Esnouf RM. Further additions to MolScript version 1.4, including reading and contouring of electron-density maps. Acta Crystallogr D Biol Crystallogr 1999;55:938–940.
39. Merrit EA, Bacon DJ. Raster3D: photorealistic molecular graphics. Methods Enzymol 1997;277:505–524.
40. Persistence of Vision Development Team. POVRay—The Persistence of Vision Raytracer. http://www.povray.org/ 2002;version 3.5.
41. Brünger AT. Free R value: a novel statistical quantity for assessing the accuracy of crystal structures. Nature 1992;355:472–475.
42. Hofmann A, Wlodawer A. PCSB—a program collection for structural biology and biophysical chemistry. Bioinformatics 2002;18:209–210.